Taylor & Francis
Taylor & Francis Group

MECHANO-CHEMICAL PREPARATION AND APPLICATION OF MULBERRY-LIKE CACO$_3$/SIO$_2$ COMPOSITE PARTICLES IN SUPERHYDROPHOBIC FILMS

Xiufang Wen, Ying Liu, Zijie Xu, Jinxin Yang, Pihui Pi, Zhiqi Cai, Jiang Cheng, and Zhuoru Yang

School of Chemistry and Chemical Engineering, South China University of Technology, Guangzhou, China

□ *This study focuses on preparation of mulberry-like CaCO$_3$/SiO$_2$ composite particles with a mechanochemical method and their application in superhydrophobic films. Silicon dioxide nanoparticles were adhered to calcium carbonate microparticles to form mulberry-like composite particles through vigorous stirring, which prevented agglomeration of silicon dioxide nanoparticles and maintained their nanocharacteristics. Then, hexamethyldisilazane was employed for hydrophobic modification of the mulberry-like CaCO$_3$/SiO$_2$ composite particles. The effect of CaCO$_3$/SiO$_2$ mass ratios, stirring speed, reaction temperature, and amount of modifying reagent on morphology and lipophilicity of composite particles was studied. Moreover, the superhydrophobic films with excellent film properties were obtained by through combination of mulberry-like CaCO$_3$/SiO$_2$ hydrophobic composite particles and RTV silicon rubber. The water contact angle and sliding angle of the superhydrophobic surface were measured to be 170 ± 2.5° and 4°, respectively. This approach proves to be ideal for substantial improvement of the self-cleaning property of RTV silicon rubber anti-pollution flashover coating.*

Keywords Coating, Mechano-chemical method, Nano-micro composite particle, Superhydrophobic surface, Smart materials

INTRODUCTION

Advances in nanotechnology have stimulated the development of new biomimetic materials with micro-nanoscale binary structures and fabrication of superhydrophobic or superhydrophilic surfaces (1). A typical example of learning from nature is the creation of superhydrophobic surfaces by imitating the microstructure of lotus leaves (2). Among the various techniques

employed to fabricate superhydrophobic surfaces (3–6), assembly of the inorganic composite nanoparticle is simple and inexpensive for preparation of micro/nano dual-scale surface structure.

In general, the microstructure of the composite particle has a great influence on the performance of composite particle assembly films. To obtain composite particles with the desired microstructure, Reculusa et al. (7) prepared raspberry-like hybrid organic-inorganic materials consisting of spherical silica beads to support smaller polystyrene particles through a heterophase polymerization process. Armes et al. (8) synthesized "currant-bun" polymer-silica nanocomposite particles at high yield by homopolymerizing 4-vinylpyridine in the presence of an ultrafine silica sol using a free-radical initiator in aqueous media at 60°C. Maeda et al. (9–12) prepared novel polypyrrole-silica/tin dioxide colloidal composites by chemically polymerizing pyrrole using either $FeCl_3$ or $(NH4)_2S_2O_8$ oxidants in the presence of small colloidal silica/tin dioxide particles. Demirel et al. (13) tuned the hydrophobicity of a film by adjusting the amount of particles in the two-component system with composite particles. A sharp transition from a polymer-rich surface to a nanoparticle-rich surface was observed with an increase in the mass fraction of particles in spin-coated thin films. Tsai and Lee (14) used a layer-by-layer assembly of silica particles to prepare raspberry-like particulate films for the fabrication of superhydrophobic surfaces. Ming et al. (15) prepared a superhydrophobic film by synthesizing silica-based raspberry-like particles and binding them on an epoxy-based polymer matrix after their surface was modified with a layer of Polydimethylsiloxane (PDMS). Hao Wang et al. (16) fabricated super hydrophobic coating based on modified nano-sized calcium carbonate and ordinary polyacrylate. Super hydrophobic coating with water contact angle of 155° was obtained from modified $CaCO_3$ and the polyacrylate at their weight ratio of 8/2 through a simple procedure. However, there have been very few reports on the fabrication of superhydrophobic surfaces with simple coating methods to construct a solid surface with excellent film property, appropriate surface roughness, and low surface energy (17). Most of these reported approaches are limited by deterioration on film property, rigorous experimental conditions, multi-step processes, or complicated instruments, making it difficult to scale up the production for practical use. Therefore, the application of superhydrophobic surfaces has so far remained narrow.

In this contribution, we present a simple, robust, and effective procedure to fabricate superhydrophobic surfaces with excellent film property by employing room temperature vulcanized (RTV) silicone rubber and mulberry-like composite particles based on the our early research (18). Because SiO_2 and $CaCO_3$ particles are reinforced fillers and semi-reinforced fillers of RTV silicone rubber, mulberry-like composite particles

were prepared by adhering silicon dioxide nano-particles to microcalcium carbonate microparticles by vigorous stirring to prevent the agglomeration of the former. Then hexmethyldisilazane (HMDS) was grafted on the surface of silicon dioxide through chemical bonds. The hydroxyl groups on the silicon dioxide particles surface were replaced by $-Si(CH_3)_3$ groups with high steric hindrance. For improved film property, the superhydrophobic surfaces were then obtained, first, by a spray of RTV silicon rubber without composite particles onto a clean glass substrate, followed half an hour later by a spray of the RTV silicon rubber with mulberry-like composite particles on top of it. This approach is ideal to obtain enhanced hydrophobicity of the RTV silicone rubber anti-pollution flashover coating and improve the self-cleaning property by preventing the accumulation of contaminants on the surface of the insulators.

EXPERIMENTAL SECTIONS

Preparation of Hydrophobic Mulberry-Like Superhydrophobic Composite Particles

20-g precipitated calcium carbonate (calcite, fusiform, particle sizes is 0.8–1 μm, provided by Fujian Longpu Light Calcium Carbonate Factory, China) and various weights of SiO_2 (particle sizes: 30 ± 5 nm, purchased from Zhejiang Hongsheng Nano-material Co. Ltd, China) were introduced in the homogenizer for a 10-min premixing at 1000 rpm, and then with vigorous stirring at 4500 (or 6500, 7500) rpm for 30 minutes based on the research of F.S. Li (19) and H. Honda (20), which resulted in the precursor of mulberry-like composite particles. To graft $-Si(CH_3)_3$ groups onto the composite particles, the precursor was transferred into a 500-mL flask and different volumes of HMDS were added simultaneously. The mulberry-like superhydrophobic composite particles were obtained after the mixture was stirred at 2000 rpm at different temperatures for 5 hours.

Preparation of Superhydrophobic Surfaces

The 100-g PDMS with a viscosity of 6000–20,000 mPa·s and various weights of composite particles were mixed homogeneously in a planetary mixer and admixed in succession with 15-g trimethylsilyl-terminated polydimethylsiloxane with a viscosity of 100 mPa·s, 0.2-g dibutyl tin laurate, 5-g vinyltriethoxysilane (A-151), and 5-g γ-aminopropyl triethoxysilane (A-1100) at 100–150°C for 5 h. The components were then mixed for 20 min at a reduced pressure of about 20 mbar. After that, 25–30g gasoline was added into the mixture and mixed homogeneously. In order to obtain the superhydrophobic surfaces with excellent film property, we prepared the

composite film by, first, spraying (paint spray gun, Model 30224, made by Harbor Freight Tools) the aforementioned mixture without composite particles onto a clean glass substrate, and, half an hour later, spraying the mixture with mulberry-like composite particles on top of it. Keep the spray gun nozzle vertical to the object's surface and the distance from the object being painted at 15.24cm–22.86cm during the process of spraying. The films were cured at room temperature for 2 h first and then at 50°C for 24 h. Air pressure in the compressor was kept at 30–80 PSI. The smooth RTV silicon rubber surfaces were prepared similarly except that no composite particles were added.

Characterization

The morphologies of the composite particles were examined by scanning electron microscope (SEM) supplied by LEO (LEO 1530VP). Elemental composition was characterized by energy dispersion spectrum (EDS) which is linked with the SEM. Further details on the morphology were obtained by a transmission electron microscope (TEM, JEM-100CX II, Japan) operated at 200 kV. An atomic force microscopy (AFM) (Dimension CSPM2000) was used to investigate the topography of thin film on glass. Images were acquired under ambient conditions in tapping mode using a Nanoprobe cantilever. Contact angle for water (WCA) and slide angle (SA) were measured with an OCA15 contact angle goniometer (Dataphysics Co., Germany). Each WCA and SA value was averaged from five measurements made at different positions of the film surface.

Evaluation Method of Modification Effect (21)

The effect of surface modification was evaluated by means of lipophilicity of modified $CaCO_3/SiO_2$ composite particles. The 1-g modified $CaCO_3/SiO_2$ composite particles were put into 50-mL deionized water, and then alcohol was dropped into the water until all of $CaCO_3/SiO_2$ composite particles were wetted. The lipophilicity was calculated according to the following equation:

$$\text{Lipophilicity} = \frac{V}{50 + V} \times 100\% \tag{1}$$

where V is the volume of alcohol being used.

Test Method of Basic Performances of Superhydrophobic Film

Impact resistance of the film was examined according to the Chinese national standard GB/T-1732-93, which is defined to detect the maximum

height from which the free falling 1000g counter weight would not destroy the film on the tinplate. The analysis of adhesive attraction was conducted according to adhesive attraction test methods in GB/T9286-1998. According to that national standard, the blade is used to cut the film to make a lattice pattern on the film, with the number of both horizontal and vertical cuts being 6 in every cutting graph. The result is grade 1 when the cut line is smooth and no lattice drops off. The test was executed at least three times on one sample.

Tear strength was also examined to detect the maximum force required to tear a specimen, with the force going substantially parallel to the major axes of the test specimen. We carried out the experiment according to the Chinese national standard of GB/T529–1999. There are five specimens, with their thickness set at 2mm and the tensile speed at 50 mm/min. The strength is the average value of five test results.

Acid resistance, alkali resistance, and salt water resistance of the film were evaluated by immersion of the film into 3wt% H_2SO_4, NaOH, and NaCl aqueous solutions, respectively. The film appearance and superhydrophobicity renewing property was checked and evaluated after 48 h for H_2SO_4 and NaOH, and 7 days for salt water.

RESULTS AND DISCUSSION

Morphology of CaCO$_3$/SiO$_2$ Composite Particles

The formation mechanism and SEM image of hydrophobic mulberry-like irregular composite particle modified by HMDS is shown in Fig. 1 (18). The effect of $CaCO_3/SiO_2$ mass ratio and stirring speed on the morphology of $CaCO_3/SiO_2$ composite particles was studied and the results are shown in Fig. 2 and Fig. 3. Fig. 2 b, c, and d show the SEM images with different mass ratio at 6500 r/min while Fig. 2a is the SEM image of pure $CaCO_3$. It can be seen from Fig. 2 that some $CaCO_3$ surfaces are not covered due to insufficient silicon dioxide when the $CaCO_3/SiO_2$ mass ratio is 10:1 (Fig. 2b). The covered surface area of $CaCO_3$ increased insignificantly with the increase of silicon dioxide content (Fig. 2c and 2d). However, when $CaCO_3/SiO_2$ was up to 2:1, there was great mass of residual silicon dioxide particles around $CaCO_3$ particles.

Fig. 3 shows SEM images of $CaCO_3/SiO_2$ (mass ratio 5:1) composite particles prepared at different stirring speeds. Comparing Fig. 2c with Fig. 3 we can see that SiO_2 particles are only scattered around $CaCO_3$ particles instead of being studded on the surface when the stirring speed is 4500 r/min (Fig. 3a). The reason is that low kinetic energy is not enough to overcome interface energy between $CaCO_3$ and SiO_2 particles at low stirring speeds. When the speed is up to 6500 r/min, $CaCO_3$ particles are
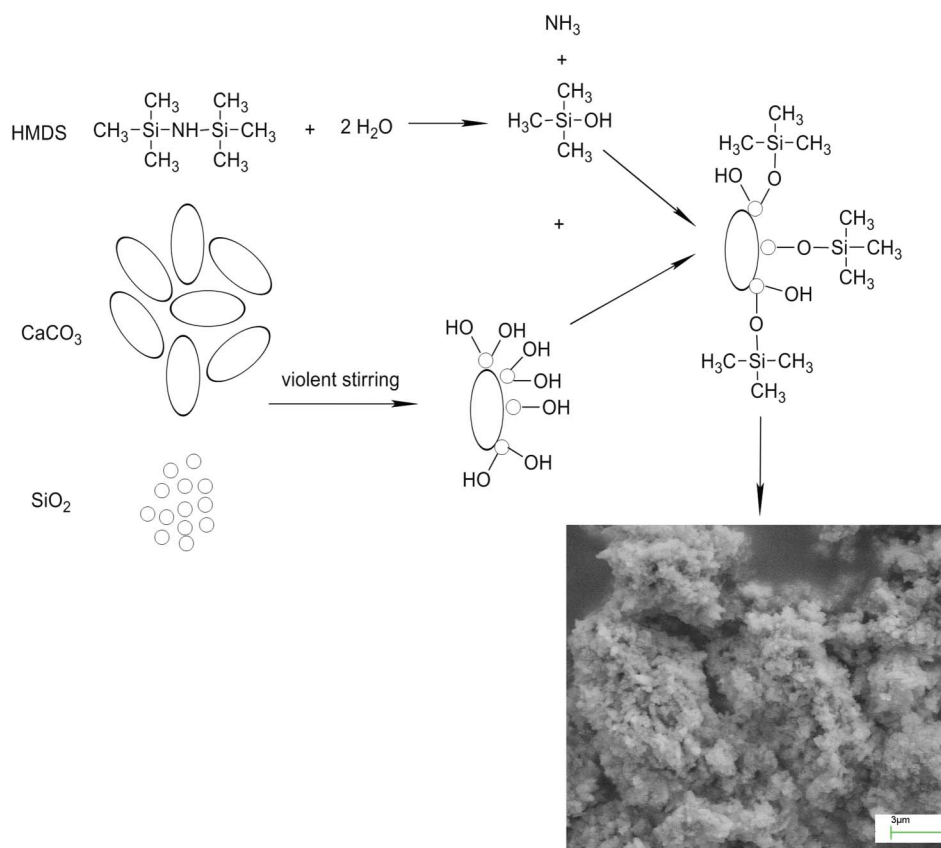
FIGURE 1 Schematic of the formation mechanism and SEM image of mulberry-like $CaCO_3/SiO_2$ composite particles.

surrounded by SiO_2 particles as shown in Fig. 2c. However, with the continuing increase of stirring speed, $CaCO_3$ particle morphology appears to be destroyed (Fig. 3b), though $CaCO_3$ could be adhesioned partially by SiO_2.

EDS was performed and the results are listed in Table 1 and 2. In Table 1 and Table 2, the reason that the mass ratio of Ca to Si is lower than the theoretical value is because of the limited detection depth of EDS on the surface of composite particles. Table 1 and Table 2 indicate that $CaCO_3$ is inside the composite particles and that the $CaCO_3/SiO_2$ mass ratio and stirring speed have the greatest effects on the composition of composite particles. The mass fraction of the silica nanoparticles relative to the calcium carbonate microparticles in composite particles increases with the increase in the mass fraction of silica nanoparticles and stirring speed. We know from Fig. 2, Fig. 3, Table 1, and Table 2 that the mulberry-like composite particles can be obtained when the mass ratio of $CaCO_3/SiO_2$ is 5:1, and the stirring speed is 6500 r/min.

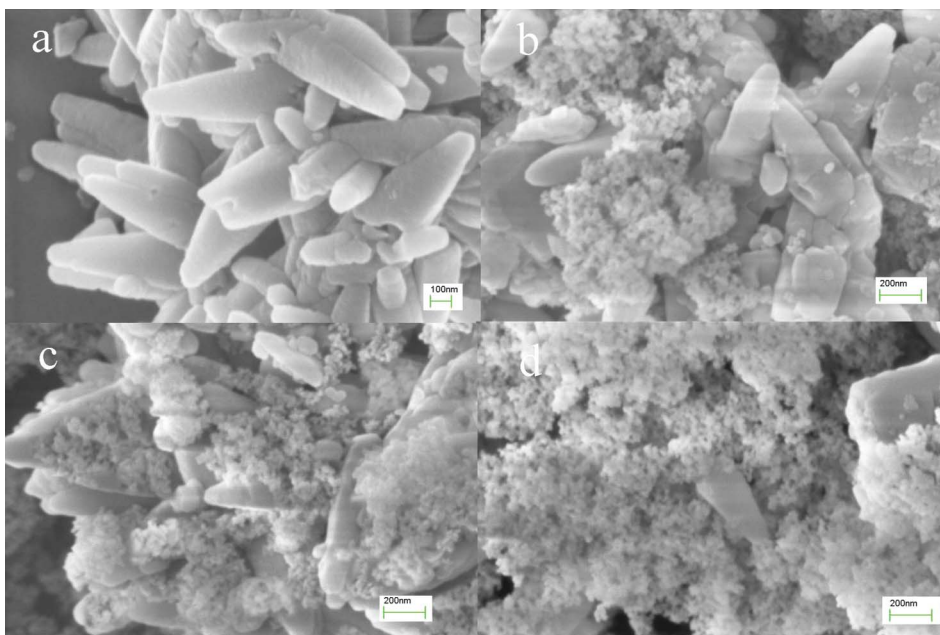**FIGURE 2** SEM images of $CaCO_3/SiO_2$ composite particles prepared with different mass ratio. (a) pure $CaCO_3$, (b)10:1, (c) 5:1, (d) 2:1.

Effect of Surface Modification on Lipophilicity of Composite Particles

The composite particles were modified with HMDS for improved lipophilicity of $CaCO_3/SiO_2$ composite particles. The effect of reaction temperature on the lipophilicity of composite particles is shown in Fig. 4. It can be seen from Fig. 4 that the lipophilicity of $CaCO_3/SiO_2$ composite particles increases initially, and then decreases with the increase in temperature. The optimal reaction temperature is then found to be about 200°C as the boiling point of HMDS is 126°C, and HMDS can vaporize to react more effectively with composite particles when the reaction temperature is higher than the boiling point of HDMS. As a result, the higher the temperature is, the higher the reactivity of HMDS with composite particles is. However, the lipophilicity of composite particles gradually decreased when the temperature was raised beyond 200°C. This happens because the hydrophobic groups grafted on particles surface are destroyed due to the thermal decomposition of organic compounds.

The lipophilicity of $CaCO_3/SiO_2$ composite particles modified at 200°C with 8mL HMDS is plotted in Fig. 5 as a function of time. As shown in Fig. 5, the lipophilicity increases quickly with reaction time. However, it stays constant at about 16 after 90 min. There is no change observed even when the
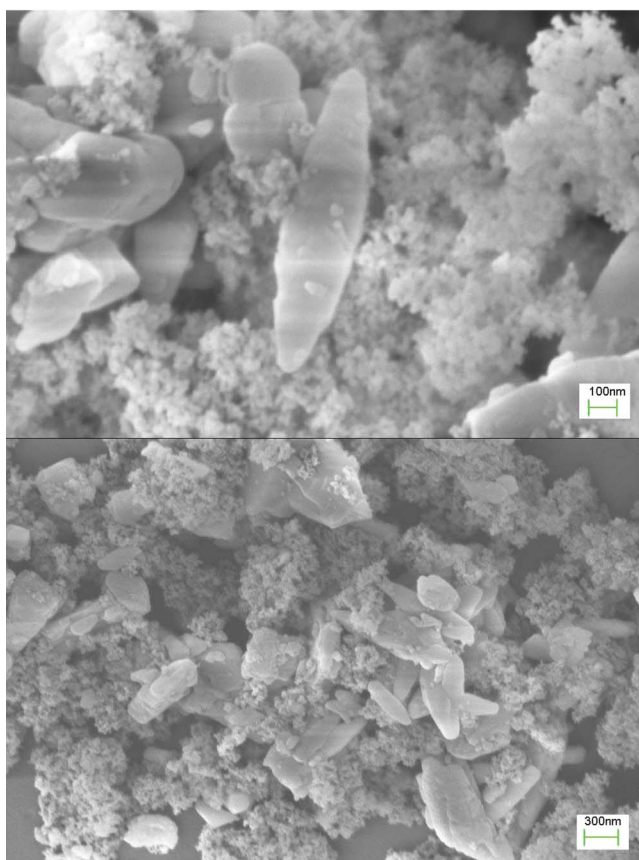
FIGURE 3 SEM images of $CaCO_3/SiO_2$ composite particles prepared at different stirring speed. (a) 4500 r/min, (b) 7500r/min.

**TABLE 1** EDS analysis of CaCO3/SiO2 composite particles prepared in different mass ratio

Element	10:1		5:1		2:1	
	Weight%	Atomic%	Weight%	Atomic%	Weight%	Atomic%
C K	13.18	20.06	15.78	23.39	19.82	28.26
O K	57.42	65.63	57.06	63.49	54.87	58.71
Si K	4.60	3.00	5.53	3.51	12.20	7.43
Ca K	24.79	11.31	21.63	9.61	13.11	5.60

reaction time is prolonged. Therefore, the reaction should be kept for at least 90 min.

Fig. 6 shows the effect of HMDS content on the lipophilicity of composite particles. The HMDS content is the ratio of volume of HMDS to the mass of composite particles. It can be seen from Fig. 6 that lipophilicity

TABLE 2 EDS analysis of $CaCO_3/SiO_2$ composite particles prepared in different stirring speed

Element	7500 rpm		6500 rpm		4500 rpm	
	Weight%	Atomic%	Weight%	Atomic%	Weight%	Atomic%
C K	22.91	31.75	15.78	23.39	9.21	14.67
O K	56.73	59.03	57.06	63.49	57.98	69.34
Si K	4.25	2.52	5.53	3.51	1.62	1.10
Ca K	16.11	6.69	21.63	9.61	31.19	14.89
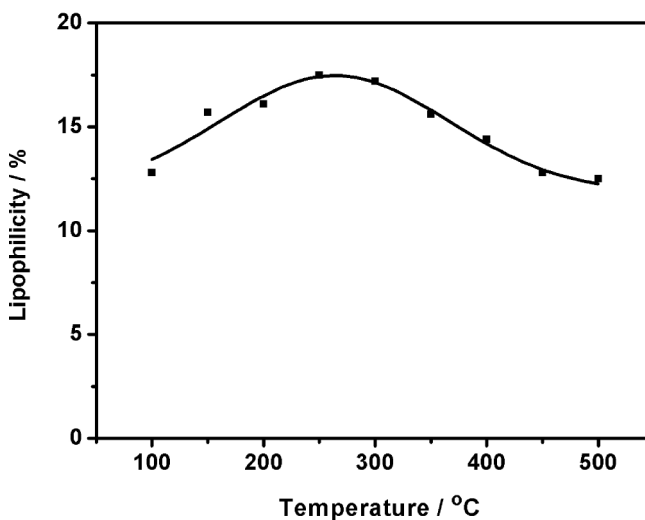
FIGURE 4 Effect of reaction temperature on the lipophilicity of modified $CaCO_3/SiO_2$ composite particles.

increased with HMDS content and reached the maximum when the content was 0.491 mL/g, and then decreased when the content of HMDS further increased, which occurs when the hydrophobic groups $-Si(CH_3)_3$ replacing the hydroxyl groups on the surface of composite particles can enhance the lipophilicity of composite particles. However, the amount of HMDS that reacted with the surface hydroxyl groups is limited, and superfluous HMDS and their hydrolysate silanol would be absorbed on the particle's surface, leading to the observed slight decrease in lipophilicity due to hydroxyl groups of silanol.

Application of Mulberry-Like $CaCO_3/SiO_2$ Composite Particle in Superhydrophobic Film

The performance of superhydrophobic surfaces with mulberry-like $CaCO_3/SiO_2$ composite particle and RTV silicon rubber is shown in Table 3.
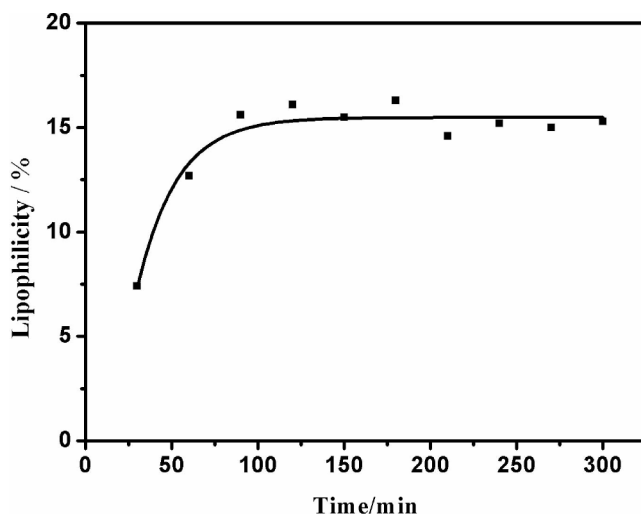
FIGURE 5 Effect of reaction time on the lipophilicity of modified $CaCO_3/SiO_2$ composite particles.

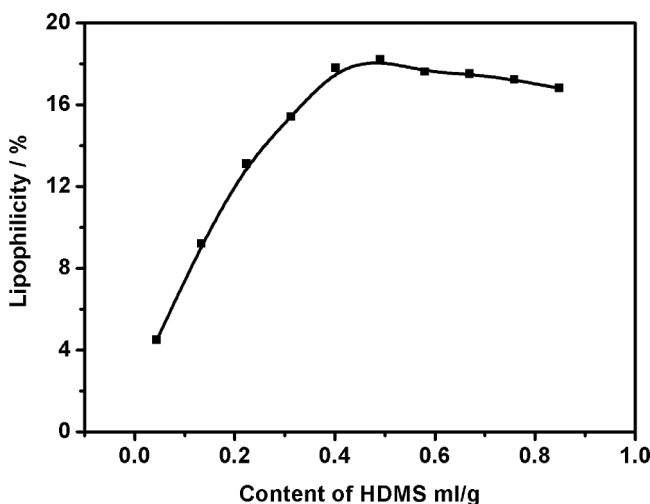**FIGURE 6** Effect of HMDS content on the lipophilicity of modified $CaCO_3/SiO_2$ composite particles.

The film property of composite film is remarkable, which makes it possible for this superhydrophobic film to be applied for RTV anti-pollution flashover coating.

To assess the effect of surface structure on the wettability of films, we measured the SEM and AFM images of film, WCA, and slide angles (SA) on the surfaces. The WCA, SEM, and AFM images of the films without and with $CaCO_3/SiO_2$ hydrophobic composite particles (sample A and B), with SiO_2 hydrophobic particles only (sample C), and with $CaCO_3$ hydrophobic

TABLE 3 Basic performances of composite film

Item	Tested Result	Standard of RTV Coating
Adhesion	1 grade	No less than 2 grade
Impact resistance	50 kg·cm	50 kg·cm
Tear strength	25kN/m	No less than 3kN/m
Acid resistance (3wt% H_2SO_4, 48h)	Film appearance no change, and renewing superhydrophobicity after 22 h	Film appearance no obvious change
Alkali resistance (3wt% NaOH, 48 h)	Film appearance no change, and renewing superhydrophobicity after 17 h	Film appearance no obvious change
Salt water resistance (3wt% NaCl, 7 days)	Film appearance no change, and renewing superhydrophobicity after 15 h	Film appearance no obvious change

particles only (sample D) are shown in Fig. 7a, 7b, 7c, and 7d, respectively. It can be seen from Fig. 7b and Table 3 that the WCA of sample B is approximately 170° and the SA is ultra-low, approximately 4°. In contrast, the WCA of sample A, sample C, and sample D were 109°, 133°, and 143°, respectively. The 5-mL water drop on the composite film will not slide from those surfaces even when the surfaces are completely vertical.

The SEM image of sample A is flat in Fig. 7a. Similar information can be obtained from the corresponding AFM image. Fig. 7c clearly shows that these rough structures of the film of sample C are made of SiO_2 nanoparticles (20–30nm). The morphology of sample D observed by SEM and AFM are shown in Fig. 7d, where only microscale structure (around 1–2μm) is seen. Such microparticle-based rough surface is attributed to $CaCO_3$ microparticles. When the mulberry-like composite particles are combined into the RTV silicon rubber system (sample B), the topographic image shows a two-level structure (Fig. 7b). The micrometer-level convexes, with a diameter from 200nm to 1μm, are attributed to mulberry-like composite particles, and the diameter of micrometer-level convexes depends on the orientation of $CaCO_3$. The magnified SEM image of the microconvexes shows that the microconvexes consist of many nanoparticles (20–30nm) (Fig. 7b).

The results of AFM images preliminary quantitative analysis, such as root-mean-square roughness (Sq which gives the standard deviation of the height values), surface roughness factor (r, r = 1 + Sdr, Sdr is surface area ratio, which is the ratio between the interfacial and projected areas), and mean roughness (Ra), were obtained from AFM software analysis in Table 4. For the films preparation with nano SiO_2 particles, microscale $CaCO_3$ particles, mulberry-like composite particles, and without composite particles, the roughness factors are 1.52, 1.21, 2.27, and 1.08, Sq are 224, 241, 372, and 68nm, respectively. The surface topography of those particular films demonstrated that a dual-scale surface structure could also be constructed using these mulberry-like particles. High WCA of composite film has been attributed to this irregular-sized hierarchical structure resembling
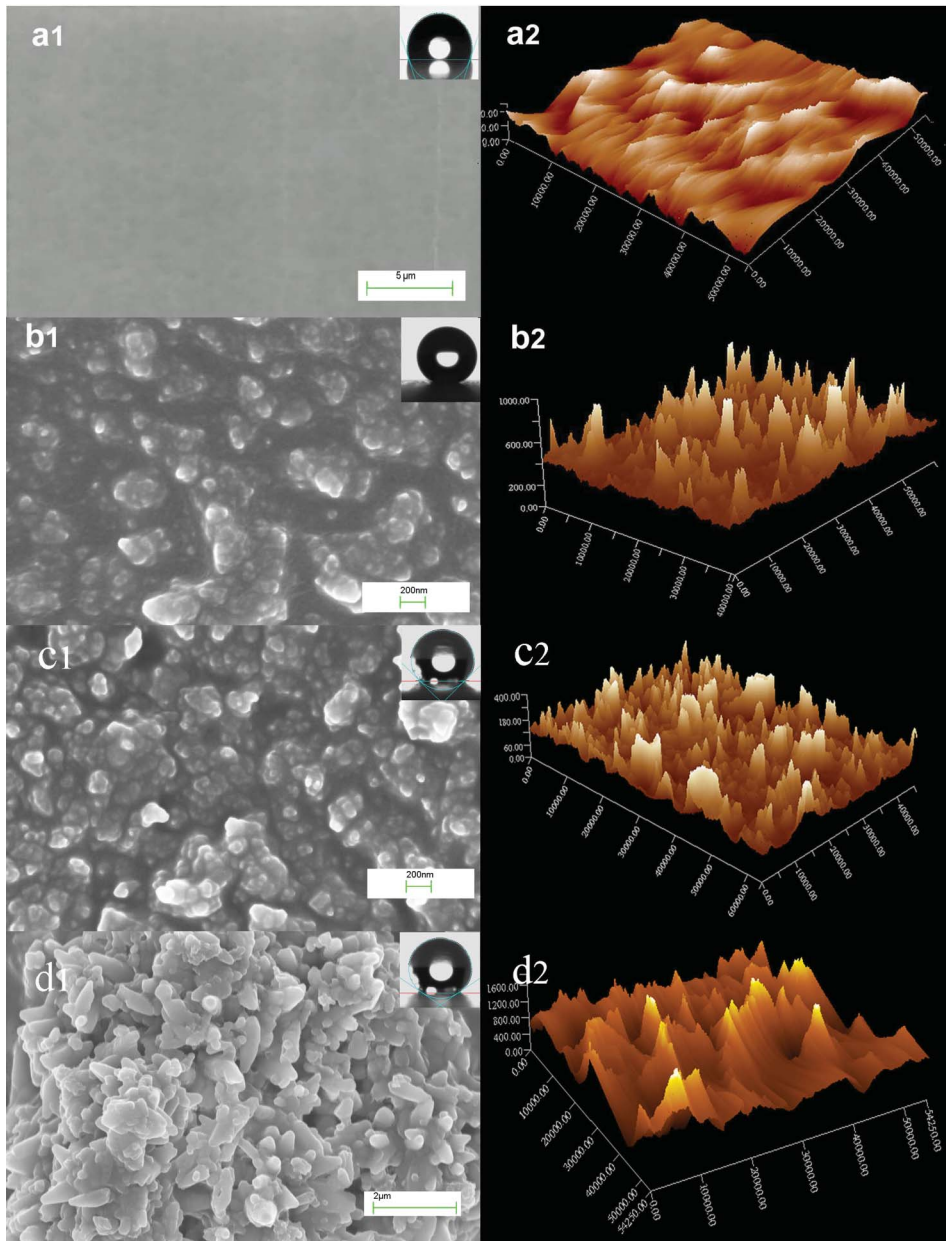
FIGURE 7 SEM and AFM images of thin films: (a) without $CaCO_3/SiO_2$ composite particles, and (b) with $CaCO_3/SiO_2$ composite particles (c) with SiO_2 particles, (d) with $CaCO_3$ particles coating surface prepared by spray (color figure available online).

TABLE 4 Roughness parameters for samples

Samples	Sa (Roughness Average)/nm	Sq (Root Mean Square)/nm	Sdr (Surface Area Ratio)	r
A	15.1	19.9	8.28	1.08
B	329	374	127	2.27
C	145	224	51.5	1.52
D	177	241	20.6	1.21

the surface of a lotus leaf on the surface of film with mulberry-like composite particles (22).

CONCLUSIONS

A mechanochemical method has been successfully applied to prepare mulberry-like composite particles with silicon dioxide nanoparticles adhered to the surface of calcium carbonate microparticles. The hydrophobicity of composite particles increased remarkably when HMDS was employed for hydrophobic modification of these composite particles. The optimal technical parameters from our experiments are as follows: mass ratio of $CaCO_3/SiO_2$ at 5:1, stirring speed at 6500 r/min, the content of HMDS at 0.491 ml/g, the modification reaction kept at 200°C for at least 90 min or slightly longer. Superhydrophobic films with WCA $170 \pm 2.5°$ and good performance are fabricated by the mix of the mulberry-like $CaCO_3/SiO_2$ hydrophobic composite particles and RTV silicon rubber through spraying. This approach is very suitable for enhanced hydrophobicity of RTV silicone rubber anti-pollution flashover coating and prevent accumulated contamination on the surface of the insulators.

ACKNOWLEDGMENTS

REFERENCES

[1] Sun, T.L., Wang, G.L., Feng, L., Liu, B.Q., Ma, Y.M., Jiang, L, and Zhu, D.B. (2004) *Angew. Chem. Int. d.*, 43:357.

[2] Shang, H.M., Wang, Y., Limmer, S.J., Chou, T.P., Takahashi, K., and Cao, G.Z. (2005) *Thin Solid Films*, 472:37.

[3] Shibuichi, S., Onda, T., Satoh, N., and Tsujii, K. (1996) *J. Phys. Chem.*, 100:19512.

[4] Nakajima, A., Abe, K., Hashimoto, K., and Watanabe, T. (2000) *Thin Solid Films*, 376:140.

[5] Tadanaga, K., Katata, N. and Minami, T. (1997) 80:3213.

[6] Tadanaga, K., Katata, N., and Minami, T. (1997) *J. Am. Ceram. Soc.*, 80:1040.

[7] Reculusa, S., Poncet-Legrand, C., Bourgeat-Lami, E., et al. (2002) *Chem. Mater.*, 14:2354.

 [8] Percy, M.J., Barthet, C., Lobb, J.C., Khan, M.A., Lascelles, S.F., Vamvakaki, M., and Armes, S.P. (2000) *Langmuir*, 16:6913.
 [9] Maeda, S., and Armes, S.P. (1993) *J. Colloid Interface Sci.*, 159:257.
[10] Maeda, S., and Armes, S.P. (1994) *J. Mater. Chem.* 4:935.
[11] Maeda, S., and Armes, S.P. (1995) *Synth. Met.*, 69:499.
[12] Maeda, S., and Armes, S.P. (1995) *Chem. Mater.* 7:171.
[13] Yü ce, M.Y., Demirel, A.L., and Menzel, F. (2005) *Langmuir* 21:5073.
[14] Tsai, H.J., and Lee, Y.L. (2007) *Langmuir*, 23:12687.
[15] Ming, W., Wu, D., van Benthem, R., and de With, G. (2005) *Nano Lett.*, 5:2298.
[16] Wang, H., Tang, L.M., Wu, X.M., Dai, W.T., and Qiu, Y.P. (2007) *Appl. Surface Sci.*, 253:8818.
[17] Abdelsalam, M.E., Bartlett, P.N., Kelf, T., and Baumberg, J. (2005) *Langmuir*, 21:1753.
[18] Yang, J.X., Pi, P.H., Wen, X.F., Zheng, D.F., Xu, M.Y., Cheng, J., and Yang, Z.R. (2009) *Appl. Surface Sci.*, 255:3507.
[19] Li, F.S., and Yang, Y. (2002) *Nano/micron Composite Technology and Application;* National Defense Industry Press: Beijing.
[20] Honda, H., Kimura, M., Honda, F., Matsuno, T., and Koishi, M. (1994) *Colloids Surfaces A*, 82:117.
[21] Wang, G.H., and Li, D.H. (2005) *Paint Coatings Industry*, 35:10.
[22] Feng, Q.X.J., Feng, L., Jin, M.H., Zhai, J., Jiang, L., and Zhu, D.B. (2004) *J. Am. Chem. Soc.*, 126:62.